TECHNICAL REVIEW

No. 2 — 1983

Contents

SYSTEM ANALYSIS and TIME DELAY SPECTROMETRY (Part II)

by

H. Biering, M.Sc.
and
O.Z. Pedersen, M.Sc.

ABSTRACT

Time Delay Spectrometry (TDS) is a relatively new method for measurement of system response. Based on a linear sine sweep it optimizes measurement performance eliminating some earlier drawbacks of swept measurements. By its very nature this method tempts us to adopt an identical complex description in the time and frequency domains. A general theoretical background for this description was given in Part I of this article.

The present part deals specifically with the TDS technique and its practical implementation in the B & K Time Delay Spectrometry System Type 9550. It is shown that the analysis carried out is similar, although not identical to standard correlation analysis techniques. The theoretical limitations of the techniques are evaluated from an intuitive point of view and are confirmed by a more rigorous mathematical approach.

SOMMAIRE

La Spectrométrie à Filtrage Décalé (TDS) est une méthode relativement récente pour la mesure de la réponse des systèmes. Fondée sur un balayage sinusoïdal linéaire, elle optimise la mesure des performances en éliminant quelques inconvénients des mesures par balayage. De par sa nature même, cette méthode nous incite à adopter une description complexe identique dans les domaines temps et fréquence. Les éléments de base théoriques de cette description ont été donnés dans la partie I de cet article.

Cette deuxième partie traite plus spécialement de la technique TDS et de sa réalisation pratique dans le Système B & K de Spectrométrie à Filtrage Décalé Type 9550. Elle montre que l'analyse effectuée est similaire, sans être identique, aux techniques standard d'analyse par corrélation. Les limites théoriques des techniques sont évaluées de façon intuitive et confirmées par une approche mathématique plus rigoureuse.

ZUSAMMENFASSUNG

Time Delay Spectrometry (TDS) ist eine relativ neue Methode zur Messung der Eigenschaften von Systemen. Die Messung basiert sich auf einer linearen Sinusdurchstimmung und ist optimiert, so daß einige der Nachteile durchgestimmter Messungen eliminiert sind. Die Methode verleitet uns dazu, dieselbe komplexe Darstellung im Frequenz- sowie im Zeitbereich zu benutzen. In Teil 1 des Artikels wurde der theoretische Hintergrund für diese Beschreibung gegeben.

Der vorliegende Teil beschäftigt sich im wesentlichen mit der TDS-Technik und der praktischen Anwendung im Brüel & Kjær TDS-Meßsystem 9550. Es wird gezeigt, daß die verwendete Technik der normalen Korrelations-Analysentechnik ähnlich, jedoch nicht mit ihr identisch, ist. Die theoretischen Begrenzungen dieser Methoden werden zunächst intuitiv beurteilt und durch gründlichere mathematische Methoden bestätigt.

5. TDS – Principle

In this section an intuitive description of the TDS principle with little use of mathematics will be given. The general limitations of any time selective technique was discussed in Section 4. Here the limitations specific to the TDS technique will be discussed in some detail, and guidelines in the choice of measurement parameters given. A more rigorous mathematical treatment can be found in Section 7.

5.1. Excitation Signal

The excitation signal used in conjunction with the TDS technique is a **linear** sweep with constant amplitude. For convenience the amplitude can be set to unity. The sweep starts at a frequency f_a ($t = 0$) and stops at a frequency f_b ($t = T_S$), T_S being the total sweep time, yielding a frequency range of $F = f_b - f_a$. For simplicity f_a or f_b can be chosen to be zero. If this is done the sweep is fully characterised by the frequency range F and the sweep time T_S. The unity amplitude linear sweep with a starting frequency equal to zero may then be written as:

$$u(t) = \cos(\theta) = \cos\left(\pi t^2 \frac{F}{T_s} \right) \tag{5.1}$$

(ignoring the initial phase)

The instantaneous frequency f_i is defined as the time derivative of the phase θ

$$f_i = \frac{1}{2\pi} \frac{d\theta}{dt} \tag{5.2}$$

and the sweep rate S as the time derivative of f_i

$$S = \frac{df_i}{dt} = \frac{1}{2\pi} \frac{d^2\theta}{dt^2} \tag{5.3}$$

Differentiation of the phase term in 5.1 yields

$$f_i = t \cdot \frac{F}{T_S} = t \cdot S \tag{5.4}$$

$$S = \frac{F}{T_s} \tag{5.5}$$

It is seen that the sweep rate S becomes constant (time independent) and that the instantaneous frequency f_i varies linearly with time – hence the notation linear sweep.

A rapid sweep is often referred to as a "chirp". This terminology is avoided here. Although, the TDS technique **allows** a fast sweep, the sweep does not **have** to be fast – in theory the sweep rate S can be chosen arbitrarily small. Furthermore, as will be seen, it is necessary to consider other parameters of the measurement than those defining the sweep in order to determine whether or not the sweep is indeed too fast.

Apparently 5.4 violates the uncertainty principle of section 4.2 which stated that we cannot give a joint frequency and time domain description with infinite accuracy in both domains. However, the instantaneous frequency of (5.4) is **not** frequency in the Fourier sense. We are just

taking the liberty to define a frequency-like parameter. Strictly speaking we should rather use the term "the derivative of the time domain phase". As instantaneous frequency, as defined above, under certain circumstances has some resemblance with frequency in the Fourier sense, we will use the definition anyway – keeping in mind that f_i is really a time domain description of the signal.

According to Fig.3.17 equation (5.1) and (5.2) may also be considered to be just a prescription that converts frequency into time of on going human experience and hence a delay into a frequency shift.

This is the essence of TDS and as a **linear** sweep is used the conversion factor becomes very simple – namely equal to the sweep rate *S*.

Let us illustrate this conversion by an example. In Fig.5.1 a typical measuring situation is shown. A loudspeaker is placed along with a

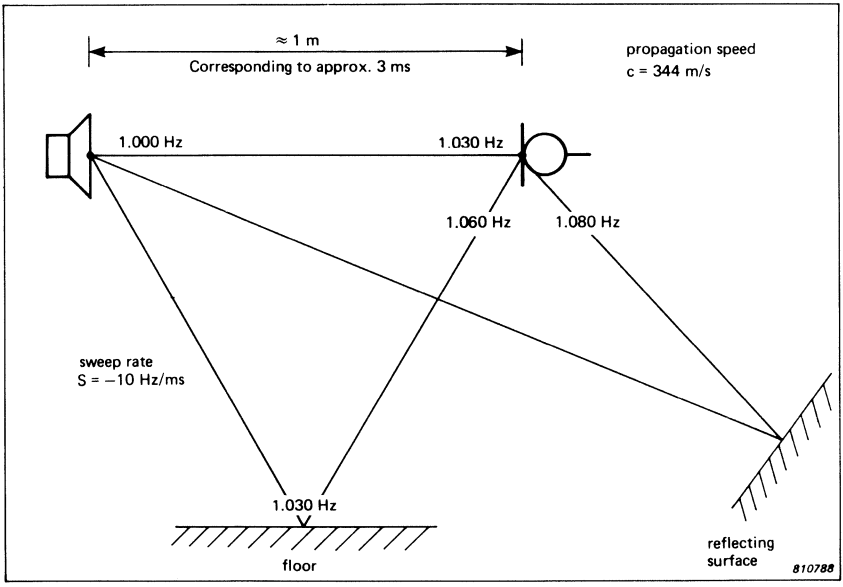

Fig. 5.1. Typical measuring situation where the free-field response of a loudspeaker has to be measured in an ordinary room. When employing a linear sweep, the various delays will be converted into frequency shifts proportional to the delay and sweep rate, S. The figure shows the frequencies present at the microphone at the moment in time when the generator is at 1000 Hz

measurement microphone in a normal room with reflecting surfaces. Only the two closest reflecting surfaces are shown. Assume that we want to measure the loudspeaker in the frequency range 20 kHz to 0 Hz ($F = -20$ kHz) and that this range is swept linearly in $T_S = 2\,s$. The sweep rate then becomes

$$S = \frac{-20\ \text{kHz}}{2\ s} = -10\ \text{Hz/ms} \tag{5.6}$$

The frequency components picked up by the microphone will now be shifted relative to the generator frequency. If for instance, at a particular moment in time, the generator frequency is at 1000 Hz the microphone frequency components can be calculated as follows. In the example shown the direct sound has to travel approx. 1 m before it reaches the microphone. With a propagation speed in air of ≈ 344 m/s this corresponds to 1/344 s ≈ 3 ms. The frequency simultaneously present at the microphone position has been transmitted from the loudspeaker 3 ms previously. At that time the generator frequency was 1000 Hz $- S \cdot 3$ ms $= 1000 - (-10) \cdot 3 = 1030$ Hz. Note that the sweep rate S is assumed negative: in the B & K TDS system, the sweep always runs from the high to the low frequencies. The same simple calculation can be made for any other travelling path. The floor reflection e.g. has to travel ≈ 2 m corresponding to a delay of 6 ms which yields a frequency shift of $6 \cdot 10$ Hz = 60 Hz and a resulting frequency of 1060 Hz. It is seen that a delay is converted into a frequency shift proportional to the sweep rate and the delay.

This domain converting property of the linear sweep has some very important consequences. We can now use all our knowledge about frequency analysis for time delay analysis. Even more important, the conventional frequency domain analyzers suddenly turns into time delay analyzers.

5.2. Method of Analysis

The discussion will later be divided into two parts, time delay analysis and frequency domain analysis. Although it theoretically suffices to perform the analysis in one of the domains and obtain the other domain representation by a subsequent Fourier Transformation, it is convenient to measure both responses in parallel.

In this way a window problem not mentioned hitherto is avoided. The problem is that the smooth frequency window often necessary to obtain a reasonable time delay response should not appear in the frequency domain. As will be clear later, in the B & K system, the Hanning frequency domain window does not affect the frequency domain display. However, as a consequence of the actual implementation the time delay window will be included in the time delay representation.

While Fig.5.1 is related to a specific moment in time Fig.5.2 shows the spectra at the microphone at 3 distinct times. Time t_1 corresponds to Fig.5.1. A little later (t_2) the spectrum has been shifted downwards in frequency. However, the relative positions of the frequency components remain unchanged. The level (and also phase) of the components

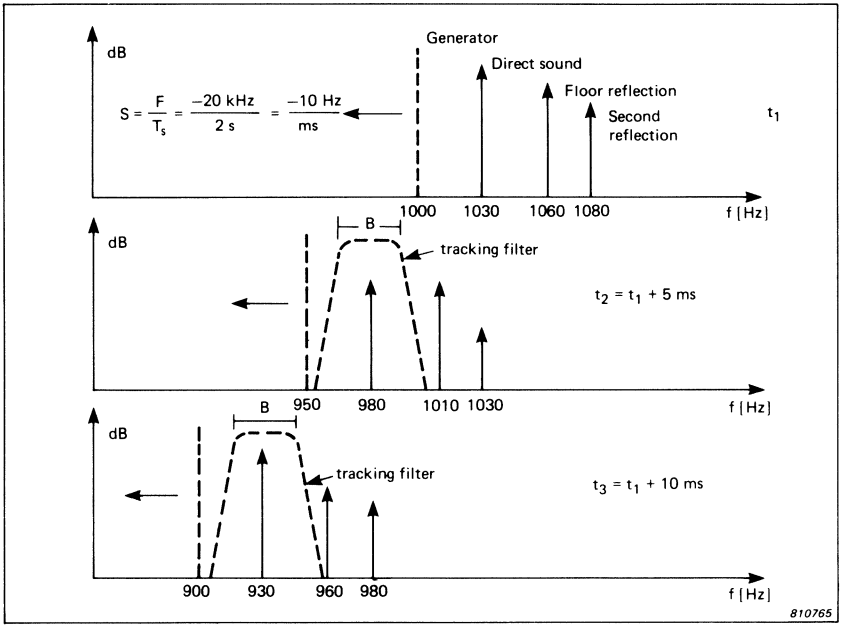

Fig. 5.2. Spectrum at the microphone corresponding to three distinct times during the sweep. t_1 corresponds to the instantaneous picture in Fig.5.1. During the sweep the whole picture will be shifted towards the lower frequencies but the relative position of the components remains unchanged. The levels of the individual components will change in accordance with the frequency responses. Here the tracking filter is tuned to measure the direct sound

will change in accordance with the frequency responses of the individual paths. At t_3 the spectrum is shifted further down and the levels have changed again.

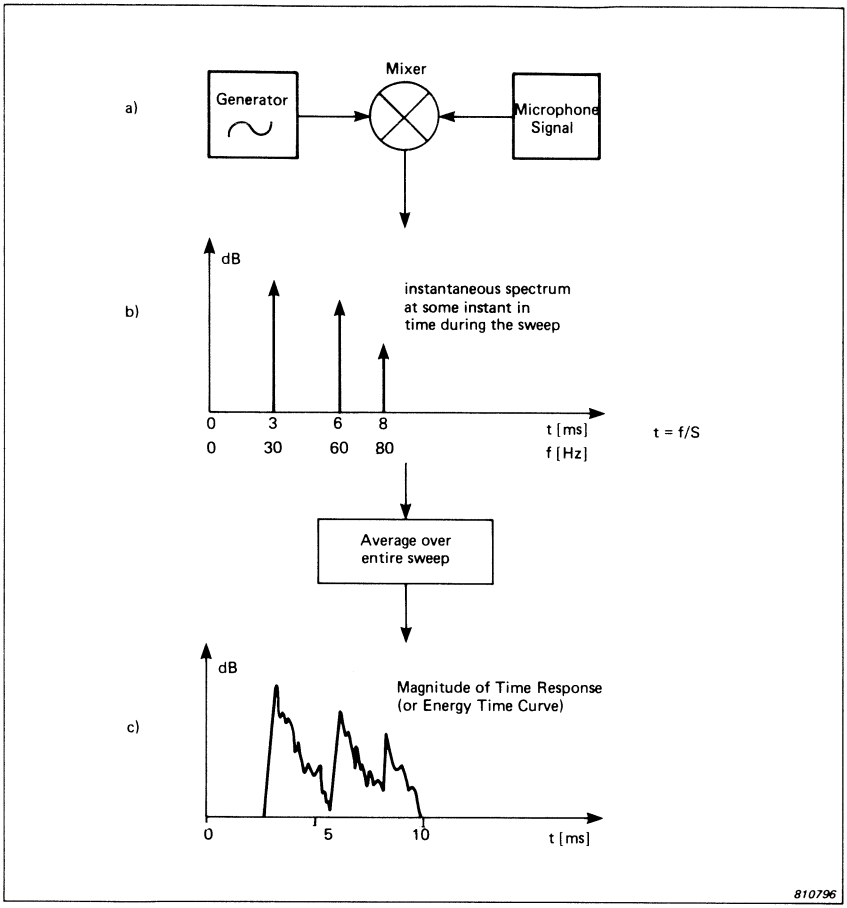

Fig. 5.3. Signal processing for obtaining the Time Response. If the microphone signal is mixed with the generator signal (a) the instantaneous spectra in Fig.5.2 will be aligned with the generator frequency at DC (b). As the individual components will be amplitude and phase modulated the spectrum will be smeared when averaged over the entire sweep (c)

It is seen that we can apply a tracking filter to the microphone signal. A proper choice of tracking filter bandwidth B and tracking filter offset f_1 will then allow us to pick out the desired part of the signal. If, as shown in Fig.5.2, we want to measure the direct sound only, the filter should be given an offset of 30 Hz and the bandwidth chosen so that the floor reflection is sufficiently suppressed. In this case B = 30 Hz would be a suitable choice. However f_1 and B can be chosen to other values as well. Setting f_1 to 60 Hz will set the filter to measure the floor reflection. In this case B should be reduced to suppress the second reflection. The tracking filter thus constitutes a time window, and the width and position can be changed by changing B and f_1 respectively. The corresponding time delay domain values are calculated by division with the sweep rate S.

As we are not concerned with the actual frequencies but only with the frequency shifts we will mix the microphone signal with the generator frequency. As a result the spectra shown in Fig.5.2 are aligned with the generator frequency at DC as shown in Fig.5.3.

5.2.1. Time Delay Analysis

Now, by making a frequency analysis of the down-mixed microphone signal, we actually perform a delay analysis. The analysis can be done serially by analog means, or better, if real-time performance is required, in parallel using an FFT–analyzer, as in the B & K system.

As the time signal output from the mixer will be amplitude and phase (frequency) modulated according to the system response, sidebands will occur in the down – mixed spectrum. However, the nature of the modulation (for causal systems) is so that the "sidebands" will only appear at positive time delay (see Fig.5.3.c). The frequency domain window is applied to the time record of the FFT analyzer only and will therefore not influence the frequency response display.

At this point, we have been forced to give up the concept of instantaneous frequency (and instantaneous spectra). We have been thinking in terms of instantaneous frequencies as representing distinct delays. However, as soon as we want to analyse the delays we must of course obey the rules of Fourier analysis.

In TDS context the time domain version of the uncertainty principle can be derived directly from the frequency domain version. As the frequency shifts are directly proportional to the sweep rate S the frequency

axis of the FFT analyzer is converted to time simply by division with S as shown in Fig.5.3.b.

The record length should be adjusted to equal the sweep time T_s. It is well known that the record length T_{FT} of the FFT–analyzer is given by the full scale frequency F_{FT} of the FFT–analyzer and the number of lines N_{FT} by

$$T_{FT} = \frac{N_{FT}}{F_{FT}} = \frac{1}{\Delta f_{FT}} \tag{5.7}$$

It is readily seen that this is just the uncertainty principle of the discrete Fourier Transform, T_{FT} being the time window and F_{FT}/N_{FT} being the frequency resolution Δf_{FT} (**not** the delay window and frequency resolution of the TDS measurement). Multiplying (5.7) by S we obtain:

$$S \cdot T_{FT} = \frac{S}{\Delta f_{FT}} \tag{5.8}$$

Remembering that frequency is converted to delay by division with S, the right hand side is seen to equal the inverse of the time resolution Δt and with $T_{FT} = T_S$ and $S = F/T_S$ the lefthand side can be rewritten

$$S \cdot T_{FT} = \frac{F}{T_S} \cdot T_S = F \qquad \text{i.e.} \tag{5.9}$$

$\Delta t = 1/F$ which is the time domain version of the uncertainty principle.

5.2.2. Frequency Response Analysis

The frequency response is measured "on-line", i.e. during the sweep. In section 7 it is shown that the filtered output signal from the mixer represents the real part of the frequency response. From the preceding discussion it will also be clear that the mixer output will be amplitude and phase modulated according to the system response. Hence the frequency response can be measured directly by measuring the envelope and phase. These are however difficult to extract, when as in Fig.5.3 the desired spectral components are positioned at or near DC. Therefore the frequency magnitude and phase responses can be detected at an earlier stage where the signal appears as a modulation of

an intermediate frequency carrier (see Section 6). In this case the phase response is obtained by comparison with a fixed carrier of the same frequency.

5.3. Sweep Rate Limitations

For a conventional unfiltered swept measurement of a frequency response there is an upper limit for the sweep rate S we can use without exceeding a given acceptable bias error. It is however, not possible to estimate this error without knowing the frequency (or delay) response in some detail. The decisive characteristics of the responses are the "peakiness" of the frequency response or the duration of the time response. The "peakiness" may be described in terms of the bandwidth of the narrowest peak in the true response, Δf_H, or the second derivative of the response (the curvature). The difficulty one is faced with in such an estimation is that one does **not** know the response in advance. Let us so far assume that we can somehow determine the duration T_H of the impulse response or the "peakiness" of the frequency response. It will be shown that when a properly chosen tracking filter and hence a time window is introduced, we are safeguarded in the sense that whatever is measured, i.e. picked up by the time window, is also measured correctly.

With no tracking filter the sweep rate S should be limited to approximately

$$S < \frac{1}{T_H^2} \leqslant \Delta f_H^2 \tag{5.10}$$

Usually $1/T_H \approx \Delta f_H$ but if a substantial amount of non minimum phase variation is present then $1/T_H < \Delta f_H$. Limitations similar to 5.10 are seen in the literature. They may differ quantitatively but not qualitatively. A rigorous derivation will not be given here, but it is intuitively clear that the response time of the system should not exceed the time it takes to sweep through the narrowest peak. With the above notation it takes $\Delta f_H / S$ to sweep through a peak Δf_H wide, and with a response time of T_H it follows

$$T_H < \frac{\Delta f_H}{S} \Leftrightarrow S < \frac{\Delta f_H}{T_H} \tag{5.11}$$

If $T_H > 1 / \Delta f_H$ it is seen that $S < 1 / T_H^2$ places a more severe restriction on S, and that $S < \Delta f_H^2$ is not sufficient. It is therefore always safe to use the duration of the time response T_H instead of Δf_H. The resulting bias error in the frequency response will of course depend on the degree to which (5.10) is fulfilled.

Let us re-define (5.10) in terms of an equivalent "time window" T_e

$$T_e = \frac{1}{\sqrt{S}} \tag{5.12}$$

Note that T_e is not a delay window in the usual sense, but the maximum duration of the time response which, for a given S, will result in a correct measurement of the frequency response.

The choice of T and T_e is very important, as their mutual relationship as well as their relation to the duration of the time delay response T_H strongly affects the quality of the measurement.

The choice is guided by two requirements:

1) The finite sweep rate S must not cause an unacceptable bias error

2) The time window T must not segment the selected part of the time response.

The first of these requirement implies that the duration of the selected part of the time response should not extend beyond T_e. The second requirement was discussed in Section 4 as it is in no way specific to the TDS technique.

If no tracking filter is used, no time window, at least not a well defined one, is present. In this case we must make sure that T_e is larger than the duration T_H of the time response.

If on the other hand a tracking filter with bandwidth B is used, and hence a time window with width $T = B / S$, then it is sufficient that T_e is chosen larger than T, as the duration of the time response will now be limited by T.

This choice of T_e in relation to T, which is characteristic for the TDS technique, is in contrast to the classical filtered swept measurement where T is chosen larger than T_e. With the TDS technique the filter and time window T is first chosen with due regard to the time response as discussed in section 4.1 of Part I. Then T_e is chosen so that any contribution lying within T is measured correctly (i.e. $T_e > T$). As contributions outside T is excluded from the measurement, T may be seen as a time domain analogy to an anti-aliasing filter and T_e as an analogy to (half) the sampling frequency used in digital measurement techniques. This feature of TDS, the time window functioning as a time domain antialiasing device, is not necessarily common to other time selective techniques.

Returning to the classical swept measurement the equivalent time window T_e is first chosen larger than the duration T_H of the time response, and then T is chosen larger than T_e (i.e. $T > T_e > T_H$). In this approach the tracking filter is used solely as a remedy to reject noise, not as a time window, and the procedure outlined above ensures that the tracking filter does not limit the time response. The classical approach will in many cases lead to a correct measurement. However, it does not lead to optimal noise rejection, and it does not possess a sensible time window. The latter property may lead to an incorrect measurement.

The two alternative choices are illustrated below. If no segmentation is required and the duration T_H is known, both methods will give a correct measurement (see Fig.5.4), as 1) and 2) are fulfilled in both cases. TDS

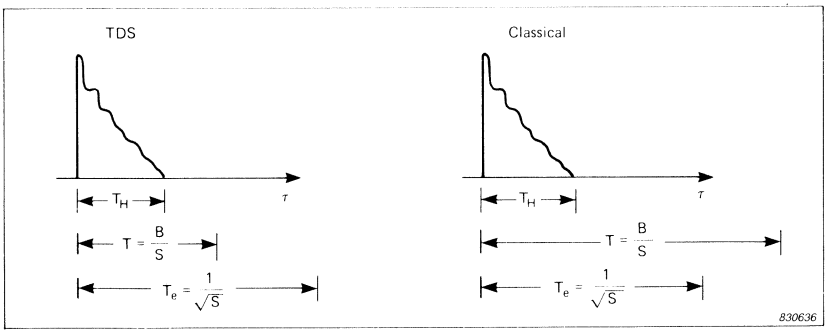

Fig. 5.4. When the duration T_H of the delay response is known, and segmentation not required TDS and the classical filtered swept measurement both provides correct measurement results

will however, give better noise rejection as is seen by rewriting T and T_e in terms of B and S.

$$T < T_e \Leftrightarrow \frac{B}{S} < \frac{1}{\sqrt{S}} \Leftrightarrow B^2 < S \quad \text{and} \quad T > T_e \Leftrightarrow B^2 > S \tag{5.13}$$

That is, for any choice of $S = F / T_S$ and hence measurement time, TDS uses a narrower filter resulting in better noise rejection.

If segmentation, is required or T_H is not known the situation in Fig.5.5 may occur. T'_H indicate the desired part of the time response (the estimated duration in the classical approach).

Also in this case noise rejection obtained with the classical approach is inferior to that obtained with TDS. Even worse, in the classical approach, the later arriving contribution in the time response is included in the measurement as it lies within T, but is not measured correctly because it extends beyond T_e.

Conclusion:

For a given time window $T = B / S$ where $S = F / T_S$ and a given frequency range F the choice

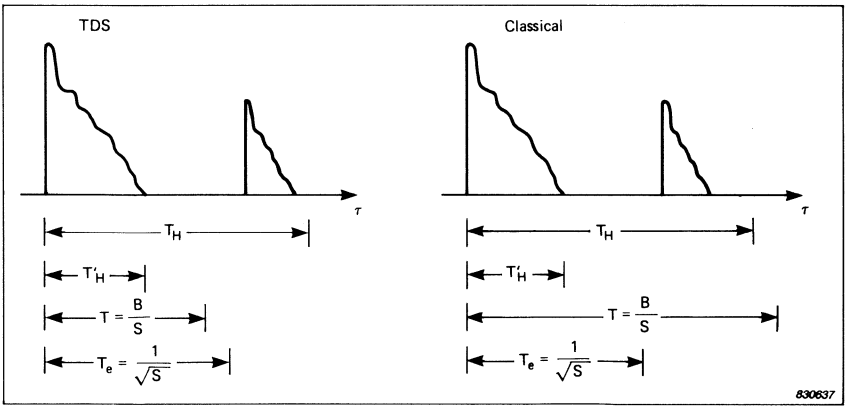

Fig. 5.5. When the delay response is not known and whenever segmentation is required, only the TDS approach leads to a correct measurement result.

$$B^2 < S \text{ (i.e. } T < T_e) \tag{5.14}$$

ensures optimal noise rejection and a correct measurement.

5.4. Choice of B and T_S

From the preceding discussion it can be seen that one degree of freedom remains in choosing the measurement parameters (B or T_S). This choice is determined by the required signal to noise ratio.

The condition $B^2 < S$ can seem strange at first glance. Apparently we can select B very small and S very large and thus suppress noise to any degree with as short a measuring time as desired ($S = F / T_S$). This is obviously not true. The condition should **always** be seen in conjunction with the frequency range F and time window $T = B / S$. Once these have been chosen, according to whatever criteria, they should be regarded as fixed. Rewriting the expression for T one obtains:

$$T = \frac{B}{S} = \frac{B \cdot T_s}{F} \Leftrightarrow F \cdot T = BT_s \tag{5.15}$$

For fixed T, it is seen that B and S decrease or increase proportionally. Recalling (5.14) an upper limit for B (and hence a lower limit for T_S) therefore exists and is given by $B^2 = S$. Substituting for S in $T = B / S$ we get

$$B_{max} = \frac{1}{T} \approx \Delta f \quad \text{and} \quad T_{S,min} = F \cdot T^2 \tag{5.16}$$

Note that the tracking filter bandwidth is always less than the frequency resolution. Note also that $T_{S,min}$ increases when the amount of information in the measurement ($F \cdot T$) is increased by increasing either F or T or both – which seems quite reasonable. The asymmetry between time and frequency is due to the fact that TDS is a serial measurement, i.e. only one point in the response is measured at a time. Assuming time invariance over a period of at least T_S, we are allowed to excite at different frequencies at different times and still get a coherent measurement. The total number of significant points being $F \cdot T$ and each point being based on the complete time range T, the minimum measuring time becomes $(F \cdot T) \cdot T = FT^2$, as also shown above.

If for instance $F = 20$ kHz and $T = 5$ ms then $F \cdot T = 100$ and $T_{s,\min} = 0{,}5$ s.

If $T_{S,\min}$ gives sufficient rejection of noise it can be used provided that the duration T_H of the time response, is not extremely large, i.e. approaching $T_{S,\min}$. In section 7 it is shown that the effective frequency window is reduced by $S \cdot \tau$. As $\tau_{\max} = T$ the relation

$$T << T_S \tag{5.17}$$

ensures that this reduction will be insignificant. However, it is seen that if (5.16) is fulfilled, T_S will be larger than T by a factor of $F \cdot T$, so that any measurement containing a reasonable amount of information will also ensure (5.17). From Section 7 it will be clear that (5.16) can be ignored as regards the magnitude of the time delay representation. In this case one must still pay attention to (5.17).

If T_H is larger than T_S, and the sweep is repeated continuously, time leakage will occur, that is, signal components with delay $T_S + \tau$ will interfere with components with delay τ. This typically happens if T_H is much larger than the desired part of the time response, T. This will often be the case when measuring the free-field response of a loudspeaker in a reverberant environment. Here the reverberation time T_{60} can be considered to be in the order of T_H. (The magnitude of the time response (ETC) is actually a reverberation decay curve although it contains much more detailed information than the traditionally measured reverberation decay). For such a measurement we could have the above mentioned $T_{s,\min}$ of 0,5 s and a reverberation time of say 1 s in which case the time response will only be down by ≈ 60 dB $\cdot$ 0,5 s/1 s = 30 dB at the end of the sweep. One remedy against this type of time aliasing is to make a single sweep, otherwise we must choose $T_S > T_H$.

It is however, more likely that the sweep time T_s should be increased in order to improve the signal to noise ratio, especially as a high T_{60} usually also implies a high level of background noise. Thus averaging by increasing T_s above $T_{s,\min}$ we also prevent time aliasing. From $F \cdot T = BT_s$ it follows that B should then be decreased proportionally in order to maintain the same basic measurement (i.e. same F and T). For instance, a doubling of T_s would improve the signal to noise ratio by 3 dB. This type of aliasing is much more severe with measurement techniques that suppresses noise by averaging several consecutive measurements.

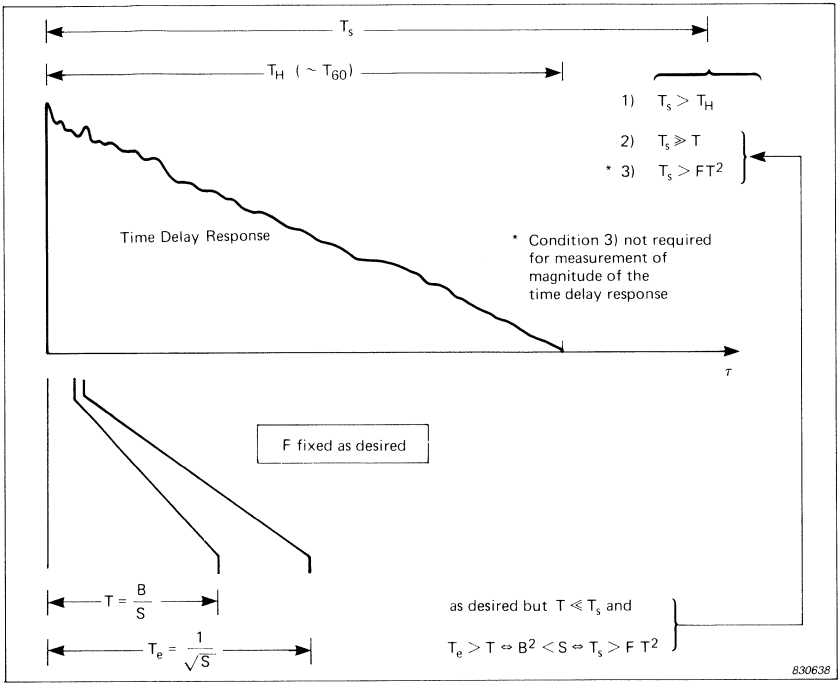

Fig. 5.6.All limitations for the TDS technique can be expressed as lower limits for the sweep time, T_s

The various limitations discussed above can be illustrated graphically (Fig.5.6). All the limitations eventually appear as minimum sweep times.

6.TDS – Implementation

The B & K TDS system is basically made up of standard instrumentation, each piece retaining its full measurement capability, the complete system thus constituting a very comprehensive measurement laboratory. The standard instruments are linked together by a special unit, the Time Delay Spectrometry Control Unit Type 5842. The Heterodyne Analyzer Type 2010 contains the Generator and tracking filter while the Distortion Measurement Control Unit Type 1902 has provision for offsetting the tracking filter. The phase of the frequency response is measured by the Phase Meter Type 2971. The time response is calculated and displayed by one of the FFT analyzers Type 2031 or 2033.

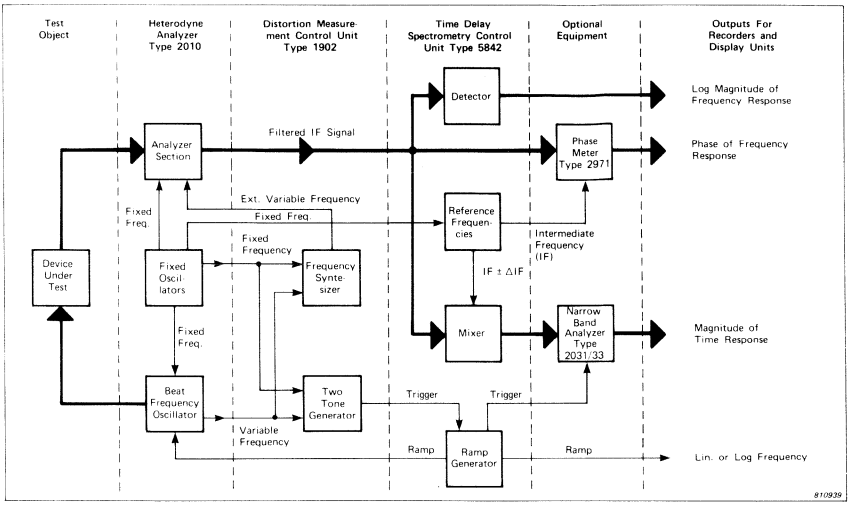

Fig. 6.1.Block diagram of the complete system. Signal paths are indicated by thick lines while reference and control signals are shown with thin lines. The signal processing in the system is based on the filtered intermediate frequency signal, IF, present at the output of the 2010 Analyzer Section when this is set to its selective mode. All response curves eventually appear as DC outputs for recorders and display units

The principle of operation of the complete TDS system is shown in the block diagram of Fig.6.1. The heavy lines indicate signal paths while the thin lines indicate reference and control signals between the various instruments.

6.1. Signal processing in the Heterodyne Analyzer Type 2010 and Distortion Measurement Control Unit Type 1902

The input for the device under test is taken from the BFO output of the Heterodyne Analyzer Type 2010. The output from the device under test is fed to the input of the Analyser Section of the 2010. Here the signal is mixed with the Ext. Variable Frequency coming from the Frequency Synthesizer section of the Distortion Measurement Control Unit Type 1902. The signal is then stepwise mixed down and filtered. Eventually it appears as a signal centred about an intermediate frequency of either

750 Hz or 30 kHz depending on the actual filter bandwidth, B. As a result the filter tracks the generator with some fixed frequency offset.

The two instruments are locked together by the fixed frequency of 1,2 MHz while the variable frequency ranging from 1 to 1,2 MHz carries the information about the Generator signal. When the Heterodyne Analyzer is operated on its own the input is mixed with the variable frequency so that the filter tracks the generator. When the Distortion Measurement Control Unit is connected, however, it takes over control of the filter position. Normally in the TDS set-up the Distortion Measurement Control Unit is operated in the intermodulation mode so that the filter can be given some fixed offset relative to the generator frequency.

A more detailed description can be found in the data sheets for Heterodyne Analyzer Type 2010 and Distortion Measurement Control Unit Type 1902.

6.2. Signal Processing in the TDS Unit

The filtered IF signal is then taken to the TDS Control Unit for further processing. A fast detector provides the output of a DC voltage proportional to the log magnitude of the frequency response. Together with a phase reference derived from the 2010 master clock the signal is fed to the phase-meter which in turn delivers a DC voltage proportional to the phase. Finally the signal is fed to the Mixer section in the TDS Control Unit.

The fact that the signal processing is based on an intermediate frequency has several advantages.

Firstly, as the detector always operates at the same frequency, the time constant of the detector can be optimised to give the fastest possible ripple-free detection. The same applies for the phasemeter.

Secondly, the signal for the reference channel of the phasemeter is simply the IF which is derived from a fixed frequency in the Heterodyne Analyzer Type 2010.

Thirdly, if the 2010 input has been mixed directly with the generator signal **and** the tracking filter center frequency is offset relative to the generator frequency to compensate a delay, the situation shown in Fig.7.2.d may occur. In this case the delay response to the left and right of the center of the delay window will overlap. Once the two parts has

been mixed it is not possible to separate them again. When the signal processing is based on an Intermediate Frequency this problem is easily overcome by offsetting the mixer frequency from the nominal Intermediate Frequency (mixer offset). As a result the center of the delay window will appear at the mixer offset frequency (Fig.7.2.e).

After mixing the signal is fed to one of the Narrow Band Analyzers Type 2031 or 2033 which calculates and displays the resulting time delay response in real time.

6.3. Control Signals

The remainder of the block diagram is concerned with control signals. The Ramp Generator delivers a fixed ramp voltage for tuning the X-drive of the recorder and display units. A variable ramp is used to tune the VCO in the Heterodyne Analyzer. In order to obtain a stable phase-curve the sweep must be started with a fixed phase relationship between the generator signal and the tracking filter signal. The low note of the two tone generator in the Distortion Measurement Control Unit when operated in the IM mode contains the necessary information. This frequency not only corresponds to the filter offset frequency but the instantaneous phase will also be the phase difference between the tracking filter and the generator. It can therefore be used to trigger the sweep start of the ramp generator. When the ramp is started, a trigger pulse is fed to the FFT Analyzer (either the Type 2031 or 2033) so that the recording starts simultaneously with the sweep.

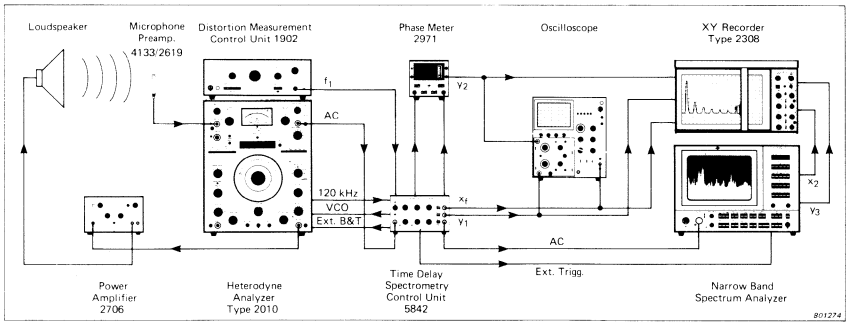

Fig. 6.2.TDS system used for loudspeaker development. The same arrangement is used for other types of measurements by exchanging the microphone and loudspeaker systems for the appropriate transducers and amplifiers

Usually the magnitude and phase of the frequency response is monitored on a variable persistance screen. All responses can be traced out via the fast X–Y Recorder Type 2308.

The complete TDS system is shown in Fig.6.2. A more detailed description of the B & K TDS system can be found in Ref.[1].

7. Signal Processing with TDS

Due to the conversion between time and frequency domains an exact analysis of the signal processing associated with Time Delay Spectrometry can seem difficult to carry out. Calculation of the Fourier integrals involved is not a simple matter when all details of practical measurements are taken into account.

To reduce difficulties in the following a pure time domain description has been evaluated. Whenever possible, however, effects encountered in the time domain are translated into frequency domain terms.

The results are obtained by combining standard correlation methods with special properties of the test signal used with TDS. Therefore the following discussion will be initiated by an introduction to these items.

7.1. Correlation

Let t represent the time of ongoing human experience. Then, if $x(t)$ is the input to a linear time invariant system and $y(t)$ is the corresponding output, they will be related by

$$y(t) = \int_{-\infty}^{\infty} g(\tau) \cdot x(t-\tau)\ d\tau \qquad (7.1.1)$$

where $g(\tau)$ is the traditional onesided, real valued impulse response.

Particularly where the input and output signals are of random nature correlation functions are often used in the calculation of $g(\tau)$. A thorough discussion of this matter can be found in Ref.[2].

For complex stationary signals we define the autocorrelation and cross correlation function as for real valued signals. Note however that $x(t)$ is replaced by $x^*(t)$, the complex conjugate of $x(t)$.

$$R_{xx}(\tau) = \overline{x^{\star}(t) \cdot x(t+\tau)} \tag{7.1.2}$$

$$R_{xy}(\tau) = \overline{x^{\star}(t) \cdot y(t+\tau)} \tag{7.1.3}$$

The test signals we apply for investigation of transfer functions, are usually limited in time. This necessitates an expansion of the basic definition substituting an average value based on the total period of excitation, T_m for the mean value of eqs.(7.1.2) and (7.1.3). By further introducing a symmetrical expression the need for separate calculations for $\tau \geq 0$ and $\tau < 0$ can be avoided:

$$R_{xx}^{T_m}(\tau) = \frac{1}{T_m} \int_{-\infty}^{\infty} x^{\star}(t - \tau/2) \cdot x(t + \tau/2)\, dt \tag{7.1.4}$$

$$R_{xy}^{T_m}(\tau) = \frac{1}{T_m} \int_{-\infty}^{\infty} x^{\star}(t - \tau/2) \cdot y(t + \tau/2)\, dt \tag{7.1.5}$$

Combining (7.1.1), (7.1.4) and (7.1.5) we obtain:

$$R_{xy}^{T_m}(\tau) = \frac{1}{T_m} \int_{-\infty}^{\infty} x^{\star}(t - \tau/2) \int_{-\infty}^{\infty} g(\gamma) \cdot x(t + \tau/2 - \gamma)\, d\gamma\, dt$$

$$= \int_{-\infty}^{\infty} g(\gamma) \frac{1}{T_m} \int_{-\infty}^{\infty} x^{\star}(t - \tau/2) \cdot x(t + \tau/2 - \gamma)\, dt\, d\gamma$$

$$= \int_{-\infty}^{\infty} g(\gamma) \cdot R_{xx}^{T_m}(\tau - \gamma)\, d\gamma$$

$$= g(\tau) \star R_{xx}^{T_m}(\tau) \tag{7.1.6}$$

All correlation functions introduced in the remaining part of this section are based on the duration of the linear sweep defined in subsection 7.2. We will therefore omit the indication of the period of excitation.

In Section 4 the effect of segmenting the time (delay) range and the frequency range was mentioned. We remind that the choice of segmentation or "windowing" is a general measuring problem not associated with any particular measuring technique. Without the loss of generality we can therefore restrict ourselves to the trivial case using rectangular weighting in both the delay and in the frequency domain.

7.2. The Linear Sweep

The term **sweep** characterizes a special class of signals that can be expressed by

$$x(t) = A(t) \cos\left(\theta_i(t)\right) \tag{7.2.1}$$

where

$A(t)$ the **amplitude modulation** and
$\theta_i(t)$ the **instantaneous phase angle**

are continuous functions of time.

We normally require that $A(t)$ be "slowly" varying compared to $\cos(\theta_i(t))$. If this condition is fulfilled we can define the **instantaneous frequency of the signal** $x(t)$ as

$$f_i(t) = \frac{1}{2\pi} \frac{d\theta_i(t)}{dt} \tag{7.2.2}$$

A **linear sweep,** which is the test signal used with TDS, is a sweep where $f_i(t)$ varies linearly with time. The fundamental parameters characterizing such a signal are the swept **frequency range,** F, and the **sweep time**, T_s.

For simplicity the deductions in this note will be based on a sweep starting at $t = 0$, where

$$f_i(0) = f_a, \quad \theta_i(0) = \theta_a \tag{7.2.3}$$

and ending at $t = T_s$, where

$$f_i(T_s) = f_b = f_a + F \tag{7.2.4}$$

For a linear sweep we will then require, that

$$f_i(t) = St + f_a, \quad 0 \leqslant t \leqslant T_s \tag{7.2.5}$$

where $S \equiv F / T_s$ denotes the **sweep rate**.

By integration of (7.2.5) one obtains

$$\theta_i(t) = \theta_i(0) + \int_0^t 2\pi f_i(\alpha)\, d\alpha + \theta_i(o)$$

$$= \pi St^2 + 2\pi f_a t + \theta_a \tag{7.2.6}$$

Using a cosine notation we can express a unity amplitude linear sweep by

$$u(t) = \begin{cases} \cos(\pi St^2 + 2\pi f_a t + \theta_a) & 0 \leqslant t \leqslant T_s \\ 0 & \text{otherwise} \end{cases} \tag{7.2.7}$$

Although physical systems can only transmit real valued time signals, any real sine or cosine sweep can be regarded as a sum of two mutually conjugate complex sweeps applied simultaneously, i.e.

$$u(t) = u_+(t) + u_-(t) \tag{7.2.8}$$

where $u_+(t) = 1/2\ e^{j[\pi St^2 + 2\pi f_a t + \theta_a]}, \quad 0 \leqslant t \leqslant T_s$ (7.2.9)

and $u_-(t) = 1/2\ e^{-j[\pi St^2 + 2\pi f_a t + \theta_a]}, \quad 0 \leqslant t \leqslant T_s$ (7.2.10)

The complex notation will be used here after as the two conjugate parts are treated separately by the measuring equipment.

7.3. Autocorrelation of the Linear Sweep

For the linear sweep $u(t)$ we find that the autocorrelation function can be separated in four parts:

$$R_{u\,u}(\tau) = \frac{1}{T_s} \int_{-\infty}^{\infty} u^{\star}(t-\tau/2) \cdot u(t+\tau/2)\, dt$$

$$= \frac{1}{T_s} \int_{-\infty}^{\infty} \left[u_+^{\star}(t-\tau/2) + u_-^{\star}(t-\tau/2) \right] \left[u_+(t+\tau/2) + u_-(t+\tau/2) \right] dt$$

$$= \frac{1}{T_s} \int_{-\infty}^{\infty} u_+^{\star}(t-\tau/2)\, u_+(t+\tau/2)\, dt + \frac{1}{T_s} \int_{-\infty}^{\infty} u_-^{\star}(t-\tau/2)\, u_-(t+\tau/2)\, dt$$

$$+ \frac{1}{T_s} \int_{-\infty}^{\infty} u_+^{\star}(t-\tau/2)\, u_-(t+\tau/2)\, dt + \frac{1}{T_s} \int_{-\infty}^{\infty} u_-^{\star}(t-\tau/2)\, u_+(t+\tau/2)\, dt$$

$$= R_{u_+ u_+}(\tau) + R_{u_- u_-}(\tau) + R_{u_+ u_-}(\tau) + R_{u_- u_+}(\tau) \qquad (7.3.1)$$

The two first terms on the right hand side of (7.3.1) are pure autocorrelation terms whereas the two last terms represent the crosscorrelation, i.e. the interaction between the two complex parts of the signal $u(t)$.

The sum of the two latter terms is calculated directly from (7.3.1). We find

$$R_{u_+ u_-}(\tau) + R_{u_- u_+}(\tau)$$

$$= \frac{1}{2\,T_s} \int_{|\tau/2|}^{T_s - |\tau/2|} \cos\left[2\pi\, S\left(t^2 + \tau^2/4\right) + 4\pi f_a t + 2\theta_a \right] dt \qquad (7.3.2)$$

This interference between the positive and the negative frequency sweeps is generally undesired. We can suppress its influence on the measurement in three different ways:

1. For the worst case situation, $f_a = 0$, and large values of T_s the sum of the cross correlation products will be limited by

$$R_{u_+ u_-}(0) + R_{u_- u_+}(0) \approx \left| \frac{1}{8\sqrt{F T_s}} \right| \qquad (7.3.3)$$

   Consequently their influence can be reduced to any desired level by increasing the sweep time.

2. The relation (7.3.3) only holds for sweeps comprising 0 Hz. When the measurement does not include very low frequencies this spurious term is strongly reduced.

3. It is readily seen that the sum of $R_{u_+u_-}(\tau)$ and $R_{u_-u_+}(\tau)$ is subject to a change of sign when θ_a is incremented by $\pi/2$. As shown below this is not the case for the pure auto correlation terms. Consequently, if a measurement is based on two successive sweeps with a phase offset of $\pi/2$ between one another the cross correlation products are totally cancelled.

For the signal $u_+(t)$ we find

$$R_{u_+u_+}(\tau) = \frac{1}{T_s} \int_{-\infty}^{\infty} u_+^{\star}(t-\tau/2)\, u_+(t+\tau/2)\, dt$$

$$= \frac{1}{4\,T_s} \int_{|\tau/2|}^{T_s-|\tau/2|} e^{j\,\pi S\left(t+\tau/2\right)^2 + 2\pi f_a\left(t+\tau/2\right) + \theta_a - \pi S\left(t-\tau/2\right)^2 - 2\pi f_a\left(t-\tau/2\right) - \theta_a\right]}\, dt$$

$$= 1/4\ e^{j2\pi f_a\tau} \cdot \frac{1}{T_s} \int_{|\tau/2|}^{T_s-|\tau/2|} e^{j2\pi S\tau t}\, dt$$

$$= 1/4\ e^{j2\pi f_a\tau} \cdot \frac{e^{j2\pi S\tau\left(T-|\tau/2|\right)} - e^{j2\pi S\tau|\tau/2|}}{j2\pi S\tau\, T_s}$$

$$= 1/4\ e^{j2\pi f_a\tau} \cdot e^{j\pi S\tau f_a\tau|\tau|} \cdot \frac{T_s-|\tau|}{T_s} \cdot \frac{e^{j2\pi S\tau\left(T_s-|\tau|\right)}-1}{j2\pi S\tau\left(T_s-|\tau|\right)} \qquad (7.3.4)$$

Similarly we obtain for $u_-(t)$:

$$R_{u_-u_-}(\tau)$$

$$= 1/4\ e^{-j2\pi f_a\tau} \cdot e^{-j\pi S\tau|\tau|} \frac{T_s-|\tau|}{T_s} \cdot \frac{e^{-j2\pi S\tau\left(T_s-|\tau|\right)}-1}{-j^{2\pi S\tau\left(T_s-|\tau|\right)}} \qquad (7.3.5)$$

The individual terms of equations (7.3.4) and (7.3.5) can be interpreted as follows:

$e^{\pm j2\pi f_a \tau}$

A simple property of the Fourier Transform is that a linearly sloping phase in one domain is equivalent to a shift of the representation in the alternative domain. In this case the slope ($\pm 2\pi f_a$) of the time delay phase is an indication of the sweep being started at the frequencies $\pm f_a$.

$e^{\pm j\pi S\tau|\tau|}$

The time delay domain phase introduced by this term is not a linear function of τ, i.e. $d(\pm \pi S\tau|\tau|)/d\tau = \pm 2\pi S|\tau|$. This means that different parts of the time domain representation are not offset by the same amount in the frequency domain representation.

$(T_s - |\tau|) / T_s$

The use of a finite test signal is the reason for this factor. It expresses the ratio between the effective integration period and the sweep time.

$$\frac{e^{\pm j2\pi S\tau(T_s-|\tau|)}-1}{\pm j2\pi S\tau(T_s-|\tau|)}$$

As long as $|\tau| << T_s$ this term is equivalent to $(e^{\pm j2\pi F\tau}-1) / \pm j2\pi F\tau$ which is the exact time domain representation for the rectangular frequency "window" ideally used for the test.

From (7.3.4–5) it is easily shown that the condition

$$|FT_s| >> 1 \qquad (7.3.6)$$

is necessary and sufficient for the uniformity of the sweep spectrum within the selected frequency range.

The denominator of the last term of (7.3.4.-5) determines the range of τ for which the total expression assumes significant values. In practice we must require that

$$|\tau| << T_s \quad \text{for any} \quad |\tau| \leq |1/F|$$

implying directly, that (7.3.6) is a necessary condition for the substitution of $T_s - |\tau|$ by T_s in the two last terms of (7.3.4.-5).

Eqn. (7.3.6) will also ensure that the second term of (7.3.4.-5) can be neglected, as

$$|S\tau^2| = \left|\frac{F}{T_s}\tau^2\right| \leq \left|\frac{F}{T_s} \cdot \frac{1}{F^2}\right| = \left|\frac{1}{FT_s}\right| \text{ for } |\tau| \leq |1/F|$$

For practical measurements $|FT_s|$ will typically be in the order of $10^3 - 10^5$.

The output signal of a system under test, $y(t)$, can be regarded as a sum of contributions from $u_+(t)$ and $u_-(t)$. We will refer to these contributions as $y_+(t)$ and $y_-(t)$ respectively.

Combining (7.1.6) and (7.3.1) we find

$$R_{uy}(\tau) = g(\tau) * \left(R_{u_+u_+}(\tau) + R_{u_-u_-}(\tau) + R_{u_+u_-}(\tau) + R_{u_-u_+}(\tau) \right) \qquad (7.3.7)$$

where $g(\tau)$ denotes the traditional impulse response of the system.

Assuming that we can neglect the interaction between $u_+(t)$ and $u_-(t)$ we obtain

$$\begin{aligned} R_{uy}(\tau) &= g(\tau) * \left(R_{u_+u_+}(\tau) + R_{u_-u_-}(\tau) \right) \\ &= R_{u_+y_+}(\tau) + R_{u_-y_-}(\tau) \end{aligned} \qquad (7.3.8)$$

indicating that we can separate the cross correlation calculations for the two complex signals $u_+(t)$ and $u_-(t)$.

For frequency domain investigations we can express (7.3.8) in terms of the corresponding cross spectra, i.e.

$$S_{uy}(f) = S_{u_+ y_+}(f) + S_{u_- y_-}(f) \tag{7.3.9}$$

where $R_{uy}(\tau) \overset{\mathcal{F}}{\leftrightarrow} S_{uy}(f)$,

$R_{u_+ y_+}(\tau) \overset{\mathcal{F}}{\leftrightarrow} S_{u_+ y_+}(f)$

and $R_{u_- y_-}(\tau) \overset{\mathcal{F}}{\leftrightarrow} S_{u_- y_-}(f)$

7.4. The Linear Sweep eliminates the need for signal storage

From the basic definition (7.1.3) it is seen that the cross correlation function is found by comparing the output signal of a system with delayed versions of the corresponding input signal. Therefore in general memory capacity for at least a period equal to the duration of the input signal must be included in the measuring instrument. The minimum amount of samples required for storage of the signal can be calculated from the sampling theorem. To store a sweep covering the frequency range F in the time T_s at least $2 \mid FT_s \mid$ real or $\mid FT_s \mid$ complex samples are needed. If the calculation procedure of the particular measuring instrument also necessitates storage of the output signal the memory requirement rises further by a factor of 2 or more.

The Brüel & Kjær Time Delay Spectrometry System Type 9550, however, utilizes the fact that a delayed version of a linear sweep can be simulated by shifting the instantaneous frequency of the original sweep by a fixed amount. Such a frequency shift is equivalent to a multiplication by $e^{j2\pi S\tau t}$, where S is the sweep rate and τ the simulated delay.

By this method the memory requirement is reduced to the minimum amount necessary to store the measured response, i.e. FT complex samples where F and T are the frequency and time delay ranges of the measurement.

The signal processing of the system is organised in several consecutive steps. As shown in Section 6 the filters of the 2010 are bandpass filters centered at different intermediate frequencies. The intermediate frequency output of the 2010 is further processed in the 5842 such that the

total **nominal** processing in these instruments is equivalent to a single multiplication with the generator signal followed by low pass filtering. The delay compensation performed by the 1902 and the display feature associated with the 5842 "Mixer Offset" can be regarded as **modifications** of this processing.

We will use the following functions to characterize the processing of the system output, $y(t)$, related to the input $u(t)$:

$u_+^\star(t)$, $u_-^\star(t)$ are the nominal multiplications taking place in the 2010 / 5842 combination

$p_+(t)$, $p_-(t)$ express the modification of the nominal multiplication for the two parts of the sweep when the 1902 is adjusted to compensate a delay, i.e.:

$$p_+(t) = p_-^\star(t) = e^{-j2\pi f_1 t}$$

where f_1 is the 1902 frequency offset.

$h(t)$ is the impulse response of the applied filter. It is convolved with the signal resulting from the previous processing. $h(t)$ is the Fourier Transform of the complex frequency response, $H(f)$, of the filter.

$q_+(t)$, $q_-(t)$ correspond to the 5842 "Mixer Offset" used to shift the time response on the 2033 display:

$$q_+(t) = q_-^\star(t) = e^{j2\pi f_o t}$$

where f_0 is the selected 5842 mixer offset frequency. $q(t)$ has no effect on the frequency domain representation.

$r(n, t)$ represents the 800 simultaneous multiplications of the 2033 input signal. The coefficients for these multiplications are given by

$$r(n, t) = e^{-j2\pi (n / T_s) t}$$

where $1 \leqslant | n | \leqslant 400$

As the final stage of the processing the 800 resulting products are integrated during the total measurement period, T_s.

To relate the frequency offsets associated with $p(t)$, $q(t)$ and $r(n,t)$ to corresponding delays we introduce the parameters

$$\xi \equiv -f_1 / S, \quad \eta \equiv -f_o / S, \quad \tau \equiv -(n / T_s) / S \tag{7.4.1}$$

and define the elementary functions

$$I(t) = e^{j\pi St^2}, \qquad o(t) = e^{j(2\pi f_a t + \theta_a)} \tag{7.4.2}$$

We can now readily derive the substitutions providing the foundation for the TDS technique. For any $t \epsilon [0, T_s]$ we find

$$u_+^{\star}(t) \cdot p_+(t) \cdot q_+(t) \cdot r(n,t) \tag{7.4.3}$$

$$= 1/2\, e^{-j2\pi f_a(\tau+\xi-\eta)} \cdot I(\tau+\xi-\eta) \cdot I^{\star}\Big(t-(\tau+\xi-\eta)\Big) \cdot o^{\star}\Big(t-(\tau+\xi-\eta)\Big)$$

and

$$u_-^{\star}(t) \cdot p_-(t) \cdot q_-(t) \cdot r(n,t) \tag{7.4.4}$$

$$= 1/2\, e^{j2\pi f_a(-\tau+\xi-\eta)} \cdot I^{\star}(-\tau+\xi-\eta) \cdot I\Big(t-(-\tau+\xi-\eta)\Big) \cdot o\Big(t-(-\tau+\xi-\eta)\Big)$$

Equation (7.4.3) is derived in Appendix B.

Using these substitutions it can be shown that the signal processing involved with Time Delay Spectrometry leads to results similar but not identical to those obtainable with standard correlation analysis. In the following sections we will make a close investigation of the TDS measurement results to provide a basis for a comparison between the two methods.

7.5. Time Response Measurements

The 2033 displays the magnitude of a complex measurement result. We will regard this result as a function of τ and refer to it as $R^{I}_{uy}(\tau)$ as it bears resemblance to the cross correlation function $R_{uy}(\tau)$.

Observing the discussion following equation (7.3.2) in subsection 7.3 we can write also $R^{I}_{uy}(\tau)$ as a sum of two contributions.

$$R^{I}_{uy}(\tau) = R^{I}_{u_+ y_+}(\tau) + R^{I}_{u_- y_-}(\tau) \tag{7.5.1}$$

The calculation of $R^{I}_{u_+ y_+}(\tau)$ and $R^{I}_{u_- y_-}(\tau)$ is based on the substitutions (7.4.3) and (7.4.4). This leads to the following results:

$$R^{I}_{u_+ y_+}(\tau) = \frac{1}{T_s}\int_0^{T_s} \Big(y_+(t)\cdot u^{\star}_{+}(t)\cdot p_+(t) \Big) * h(t)\cdot q_+(t)\cdot r(n,t)\,dt \tag{7.5.2}$$

$$= \frac{T_s}{4F^2}\left(\int_{-\infty}^{\infty} g^{I}_{\delta}\big(\tau+\xi-\eta,\gamma_0\big) * w_1\big(\tau+\xi-\eta,\gamma_0\big)\,d\gamma_0 \cdot H\Big(-S\big(\tau-\eta\big)\Big)\right)$$

$$* \; w_2\big(\tau-\eta\big)$$

and

$$R^{I}_{u_- y_-}(\tau) = \frac{1}{T_s}\int_0^{T_s} \Big(y_-(t)\cdot u^{\star}_{-}(t)\cdot p_-(t) \Big) * h(t)\cdot q_-(t)\cdot r(n,t)\,dt \tag{7.5.3}$$

$$= \frac{T_s}{4F^2}\left(\int_{-\infty}^{\infty} g^{I\star}_{\delta}\big(-\tau+\xi-\eta,\gamma_0\big) * w^{\star}_1\big(-\tau+\xi-\eta,\gamma_0\big)\,d\gamma_0 \right.$$

$$\left. \cdot\, H^{*}\Big(-S\big(-\tau-\eta\big)\Big)\right) * w^{\star}_2\big(-\tau-\eta\big)$$

where

$$g^{l}(\gamma) = g(\gamma) \cdot e^{-j2\pi f_a \gamma} \cdot e^{j\pi S\gamma^2}, \tag{7.5.4}$$

$$g_{\delta}(\gamma, \gamma_0) = g(\gamma) \cdot \delta(\gamma_0 - \gamma), \tag{7.5.5}$$

$$w_1(\gamma, \gamma_0) \overset{\mathcal{F}}{\leftrightarrow} W_1(f, \gamma_0) \tag{7.5.6}$$

$$W_1(f, \gamma_0) = \begin{cases} 1/2 \left| sgn(f-F) - sgn(f - S\gamma_0) \right|, & \gamma_0 < T_s \\ 0, & \gamma_0 \geq T_s \end{cases} \tag{7.5.7}$$

$$w_2(\gamma) \overset{\mathcal{F}}{\leftrightarrow} W_2(f) \tag{7.5.8}$$

$$W_2(f) = 1/2 \left| sgn(f-F) - sgn(f) \right| \tag{7.5.9}$$

Although neither a limitation of the technique nor the measuring equipment we have made the assumption that for the device under test $g(\gamma) = 0$ for $\gamma < 0$. This simplifies the equations that will still hold

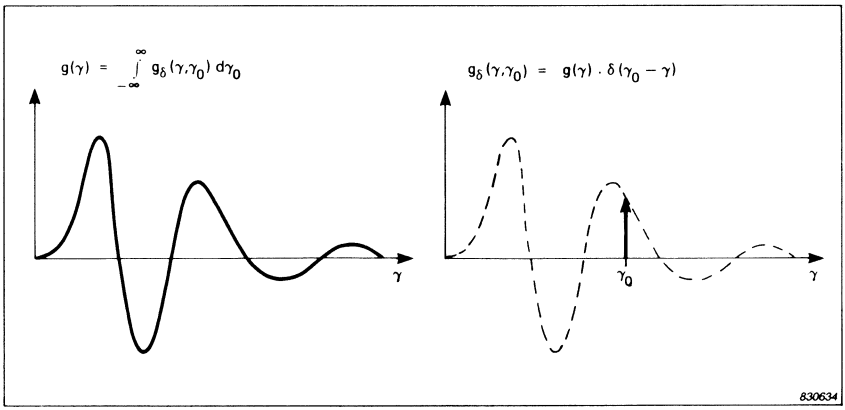

Fig.7.1. To facilitate an intuitive understanding of the signal processing it is convenient to regard the impulse response of the device under test as the sum of idealized impulse responses.

for the measurement of any physical system. The signal processing of a response depends on the actual delay γ_0. Therefore the functions $g_\delta(\gamma, \gamma_0)$ are introduced to enhance the intuitive understanding of the relationship between $g(\gamma)$ and $R^{I}_{uy}(\tau)$, see Fig.7.1.

The functions $W_1(f, \gamma_0)$ and $W_2(f)$ are rectangular window functions as the functions described in subsection 2.2, Fig.2.4 – 2.6.

The derivation of equation (7.5.2) in Appendix C uses the above definitions and assumptions. Equation (7.5.3) and similar equations allowing $g(\gamma) \neq 0$ for $\gamma < 0$ can be derived in almost the same manner.

It is readily seen that

$$R^{I}_{uy}(\tau) = R^{I\star}_{uy}(-\tau) \tag{7.5.10}$$

i.e. the real part of $R^{I}_{uy}(\tau)$ is an even function whereas the imaginary part is an odd function. This implies that $S^{I}_{uy}(f)$, the Fourier Transform of $R^{I}_{uy}(\tau)$, is a realvalued spectrum.

Furthermore, the onesidedness of $W_2(f)$ will be conveyed to both of the mutually complex conjugate spectra $S^{I}_{u_+y_+}(f)$ and $S^{I}_{u_-y_-}(f)$.

Therefore in general

$S^{I}_{uy}(f)$ is a onesided realvalued spectrum indicating that

$R^{I}_{uy}(f)$ is a symmetrical complex function with a Hilbert Transform relationship between its real and imaginary parts.

This is in contrast to the results obtained with the standard crosscorrelation technique discussed in section 7.3. From equations (7.3.4) and (7.3.5) we obtain

$$R_{u_+y_+}(\tau) = R^{\star}_{u_-y_-}(\tau) \tag{7.5.11}$$

From the definition of the Fourier Transform it is found that (7.5.11) is equivalent to

$$S_{u_+y_+}(f) = S^{\star}_{u_-y_-}(-f) \tag{7.5.12}$$

Hence

$R_{uy}(\tau)$ is a realvalued function and

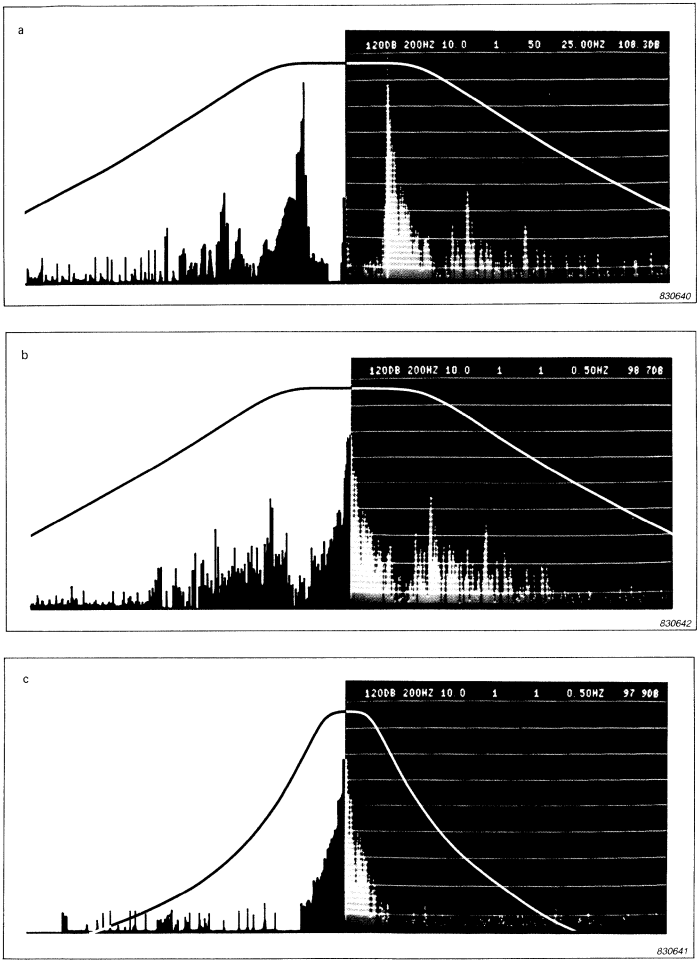

Fig.7.2. The display of the Narrowband Analyzer Type 2031/33 shows only half of the symmetrical time delay response obtained with TDS. To understand the influence of the filters (2010), the offset compensation (1902) and the mixer offset (5842) it is, however, necessary to have the total response in mind.
When the response of a loudspeaker is recorded without the use of delay compensation and mixer offset (a) the medium bandwidth filter slightly attenuates two dominating reflections.
To measure the frequency response of the direct sound from the loudspeaker further rejection of the reflections is required:

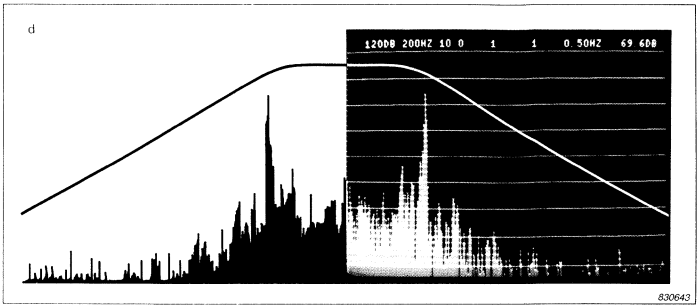

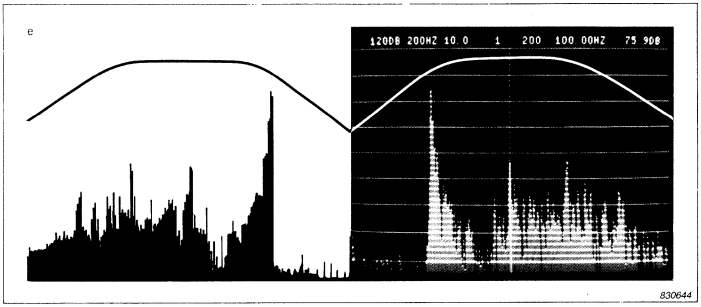

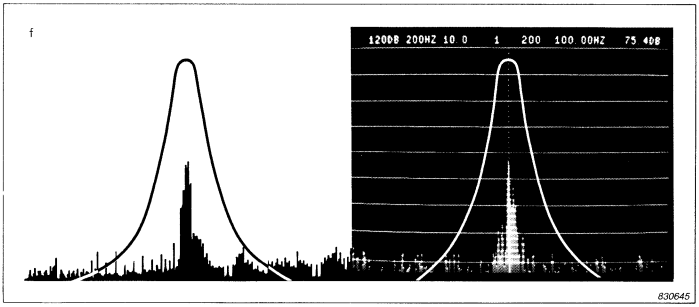

When offset compensation has been applied to center the response in the filter passband (b) the bandwidth can be further reduced (c). If alternatively the offset compensation is adjusted to equal the delay of the first reflection (d) the display is impossible to interpret due to the overlapping of the two symmetrical parts of the response. The mixer offset shifts the two parts of the response as well as the imposed "windows" away from each other. When mixer offset has been applied (e) it is easy to fine adjust the delay compensation, and to select a filter that sufficiently rejects other parts of the reponse (f)

$S_{uy}(f)$ is a symmetrical complex function. If $R_{uy}(\tau) = 0$ for $\tau < 0$ its real and imaginary part will be related by a Hilbert Transform.

These relationships were illustrated in Fig.3.4.a.–b of subsection 3.2. It is the reversed orientation of the non-symmetrical function $R_{u\_y\_}(\tau)$ that in the case of TDS inverses the time and frequency domain representation formats.

Due to the close relationship between $R^{I}_{u_+y_+}(\tau)$ and $R^{I}_{u\_y\_}(\tau)$ we will only consider equation (7.5.2) in the following discussion of the specific differences between $R^{I}_{uy}(\tau)$ and the realvalued impulse response $g(\tau)$. Initially the modified impulse response $g^{I}(\tau)$ is shifted by the amount $\eta - \xi$. If $W_1(f, \gamma_0)$ represents a sufficiently wide frequency domain "window" the following convolution with $w_1(\tau, \gamma_0)$ will yield a realvalued term proportional to $g(\tau + \xi - \eta)$ and an imaginary term equal to the Hilbert Transform thereof.

This basic time response is then multiplied by a window function with a shape related to the **frequency response** of the 2010 filter. This window is positioned symmetrically around the 5842 Mixer Offset position, η. Finally, the segmented response is frequency domain limited by convolution with the function $w_2(\tau - \eta)$.

The influence and purpose of the 2010 filters, the 1902 delay compensation and the 5842 Mixer Offset is illustrated in Fig.7.2.

For time response investigations we will normally select $\xi = \eta = 0$ and choose the filter wide enough to avoid any influence on the "raw" time response. With normalized window functions (7.5.2) can be rewritten:

$$R^{I}_{u_+y_+}(\tau) = \frac{T_s}{4} \int_{-\infty}^{\infty} \int_{-\infty}^{\infty} \left(g_\delta(\gamma, \gamma_0) \cdot e^{-j\pi f_a \gamma_0} \cdot e^{-j\pi S \gamma_0^2 \frac{T_s - \gamma_0}{T_s}} \right) \frac{W_1(\tau - \gamma, \gamma_0)}{T_s - \gamma_0} \, d\gamma \, d\gamma_0 \qquad (7.5.13)$$

From equations (7.1.6) and (7.3.4) we obtain the corresponding cross-correlation function

$$R_{u_+ y_+}(\tau) = \frac{1}{4} \int_{-\infty}^{\infty} g(\gamma) \cdot e^{j\pi f_a(\tau-\gamma)} \cdot e^{j\pi S(\tau-\gamma)|\tau-\gamma|} \cdot \frac{T_s - |\tau-\gamma|}{T_s} \cdot \frac{W_1(\tau-\gamma, |\tau-\gamma|)}{T_s - |\tau-\gamma|} d\gamma \qquad (7.5.14)$$

Apart from the mismatched scaling we can briefly explain the difference between $R^{I}_{u_+ y_+}(\tau)$ and $R_{u_+ y_+}(\tau)$ as follows:

$R^{I}_{u_+ y_+}(\tau)$ is a convolution of a modified version of $g(\gamma)$ with an idealized window function.

$R_{u_+ y_+}(\tau)$ is a convolution of the original $g(\gamma)$ with an irregular window function.

In both cases the deviation between the measurement result and the original system response can be reduced by postprocessing. For the ordinary correlation technique this involves a deconvolution of the

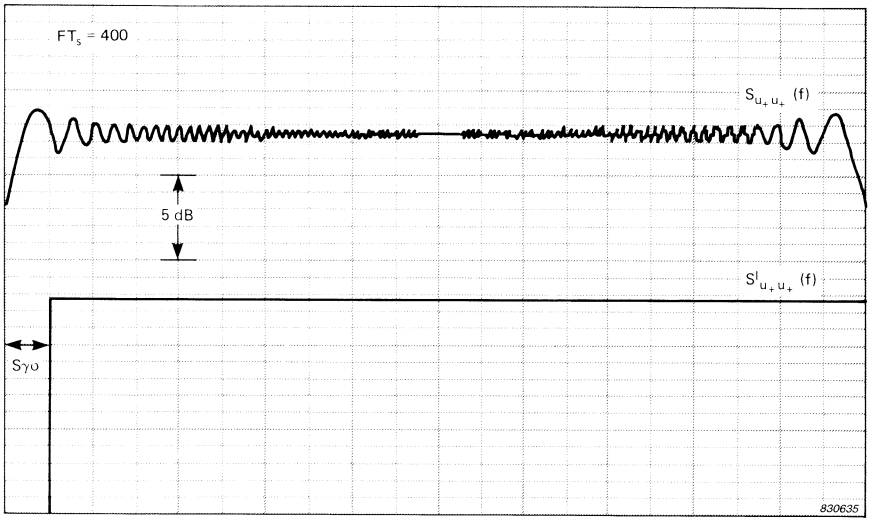

Fig.7.3. When standard correlation techniques are used the autospectrum of a linear sine sweep shows a significant amount of ripple throughout the selected frequency range. With the modified calculation procedure used for TDS measurements this is avoided. In this case, though, the selected frequency range will be reduced if the device exhibits a substantial delay.

autocorrelation function of the test signal. With TDS a simple shift of the frequency axis will normally suffice. This shift – referred to as dynamic compensation – is discussed in subsection 7.6. Typical frequency domain window functions for the two techniques are shown in Fig.7.3.

The term $e^{-j2\pi f_a \gamma_0}$ in the expression for $R'_{uy}(f)$ indicates that with the TDS technique the measured response is shifted by the starting frequency of the sweep, f_a. This frequency shift is an analogy to the delay compensation of the time response and a very useful feature for investigation of the time phase response. (Note: The time phase information can be extracted from the 2033 with a desk top calculator.) With standard correlation techniques this unwrapping of the time domain phase is not an inherent part of the processing.

By its very nature the phasor $e^{j\pi S\gamma_0^2}$ will never affect the measured time magnitude response. The time domain phase error can be reduced at will by decreasing the sweep rate. If the time phase response is investigated in the neighbourhood of ξ only, the error can be separated in three parts,

$$e^{j\pi S\gamma_0^2} = e^{-j\pi S\xi^2} \cdot e^{j2\pi S\xi\gamma_0} \cdot e^{j\pi S\left(\gamma_0-\xi\right)^2} \qquad (7.5.15)$$

The first of these is a constant phase error while the second linear term corresponds to a frequency shift by $S\xi_0$. For time phase investigations the third variable term must normally be limited by keeping $S(\gamma_0-\xi_0)^2 \ll 1$. This error term is discussed more elaborately in subsection 7.6.

The factor $(T_s-\gamma_0)/T_s$ inflicts a pure magnitude modification of the time response. In most practical cases other considerations (e.g. signal to noise ratio) will necessitate a sweep time at least an order of magnitude larger than the desired range of the time response. Therefore most often we can neglect the influence of this term.

Most characteristic for TDS is the γ_0 – dependent frequency domain window imposed on the modified response. As the useful frequency range is effectively reduced by $S\gamma_0$ we must be careful in our choice of the basic frequency range, *F*.

7.6. Frequency Response Measurements

In Section 7.5 it was stated that the time response obtained with the TDS technique was basically the Fourier Transform of the onesided real spectrum $S^{I}_{uy}(f)$. The frequency domain representation displayed by the measuring system is not, however, $S^{I}_{uy}(f)$ but the more useful complex response $S^{I}_{u_+ y_+}(f)$ presented by its magnitude and phase. The implementation of the magnitude and phase detection is outlined in section 6. It is outside the scope of this article to discuss this matter in more detail as the detectors of the present system do not contribute significantly to the discrepancies between the frequency response $G(f)$ and the measured function $S^{I}_{u_+ y_+}(f)$.

As discussed in Section 4 the decisive parameter for any frequency response measurement is the time delay range, T. Equation 7.5.2 shows that T is determined by the filter bandwidth, B of the 2010 by the relation

$$T = \left| B / \mathrm{S} \right| \tag{7.6.1}$$

This range introduces an uncertainty in the order of $1/T$ in the frequency domain representation. We define

$$\Delta f \equiv 1/T$$

and refer to Δf as the frequency resolution of the measurement.

The 5842 mixer offset is a useful feature when the time delay window is positioned using the 1902 delay compensation. However, as mentioned in Section 7.4, it does not affect the processing for the frequency domain representation.

Thus for the rewriting of equation (7.5.2) into frequency domain terms we will assume $\eta = 0$. By repeated use of substitutions of the type

$$\left(\gamma - \gamma_0\right)^2 = \gamma^2 - 2\gamma\gamma_0 + \gamma_0^2$$

and the fact, that

$$\tau + \xi = \gamma_0 \Rightarrow e^{j\pi S(\tau+\xi-\gamma_0)^2} = 1$$

we obtain

$$S^{I}_{u_+ y_+}(f) =$$

$$\left(\int_{-\infty}^{\infty} G_\delta\left(f + f_a - S\gamma_0, \gamma_0\right) e^{-j2\pi f_a \xi} e^{j\pi S\left(\xi^2-(\xi-\gamma_0)^2\right)} W_1\left(f, \gamma_0\right) d\gamma_0 \right.$$

$$\left. e^{j2\pi f \xi} \right) * h\left(f/S\right) \cdot W_2\left(f\right) \qquad (7.6.2)$$

Equation (7.6.2) describes the relationship between the original frequency response $G(f)$ and the measured crossspectrum.

The fractional response $G_\delta(f, \gamma_0)$ associated with $g_\delta(\tau, \gamma_0)$ is shifted by $S\gamma_0 - f_a$ transferring the original range of interest from f_a to f_b to the interval from $S\gamma_0$ to $F + S\gamma_0$. After a frequency independent phase modification the response is multiplied by $W_1(f, \gamma_0)$, a onesided rectangular frequency domain window ranging from $S\gamma_0$ to F. This means that the last part of the original response from $f_b - S\gamma_0$ to f_b is rejected from the measurement.

All the fractional crossspectra are now added and delay compensated by ξ (i.e. a linear increase of the frequency phase response) before the convolution with the realvalued impulse response of the filter. As the filters in the 2010 are physical devices they will have a onesided (causal) impulse response. Consequently they do not only introduce the uncertainty Δf in the frequency domain inherently imposed by the effective time window duration T. If, as in the present instrumentation, a dominating part of the filters impulse response is positioned symmetrically around a certain delay, τ_0, we will observe this as a constant frequency shift, $S\tau_0$. Typically τ_0 will be in the order of $1/B$.

Although the fractional spectra were all limited to the range given by $W_1(f, \gamma_0)$ the convolution with $h(f/S)$ can generate frequency components outside the range from 0 to F. Due to the final multiplication with the display window function $W_2(f)$ these components are disregarded in the final representation of the measurement.

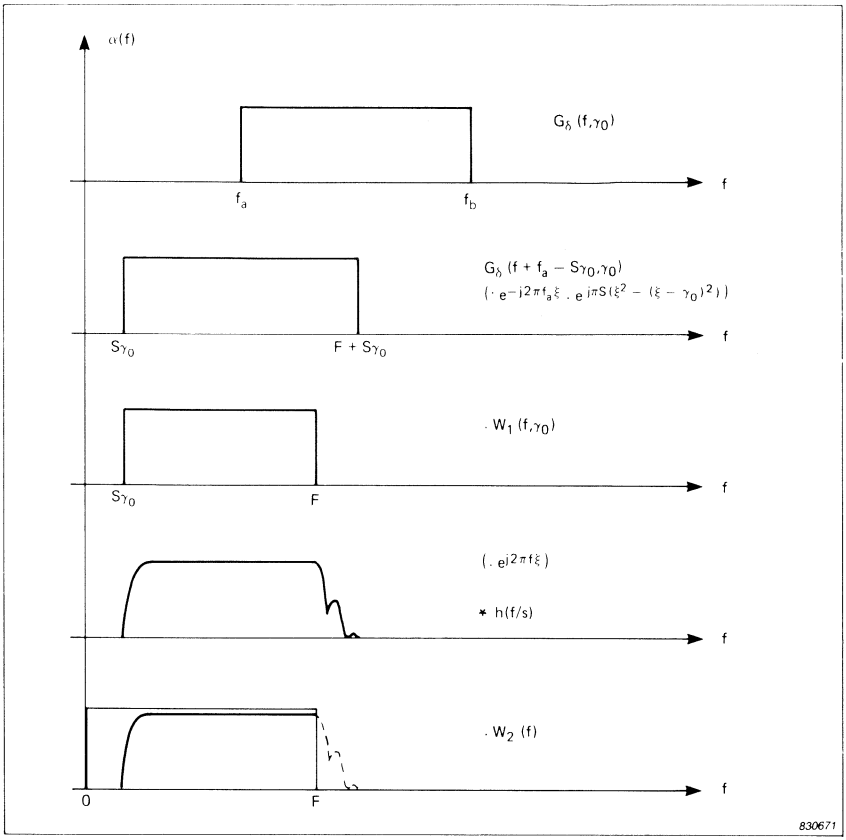

Fig.7.4. Major steps in the signal processing of $G_\delta(f, \gamma_0)$. Initially the response is shifted in frequency by the amount $S\gamma_0 - f_a$. When the window function $W_1(f, \gamma_0)$ has been imposed on the response the result is convolved with the impulse response h(f/s) of the filter before the final display window function $W_2(f)$ limits the frequency range. The response modifications indicated in parentheses cannot be observed in the figure as they influence the frequency domain phase only

Fig.7.4 illustrates some of the most important points of the signal processing.

From the above it is seen that evaluation of the original response requires a frequency compensation of the measured cross spectrum.

Normally the delay compensation, ξ, is adjusted to centre the desired part of the response in the time window. For proper analysis of the fractional response $G_\delta(f, \gamma_0)$ we select $\xi = \gamma_0$. The total shift of the frequency response then amounts to $S(\xi + \tau_0) - f_a$. Therefore we must interpret the frequency domain display as ranging from $f_a - S(\xi + \tau_0)$ to $f_b - S(\xi + \tau_0)$. Having compensated this frequency shift of the display we must further subtract the frequency independent term $\pi S(\xi^2 - f_a \xi)$ from the measured phase response.

We should, however, consider not only the fractional response $G_\delta(f, \gamma_0)$, but the integral of all the fractional responses. $G_\delta(f, \gamma)$, within the selected time range $-T/2 < \gamma - \xi < T/2$. As we are not able to compensate these responses individually we must use the average compensation $\xi = \gamma_0$.

The consequence of this average compensation is that:

a. the applied frequency compensation differs by up to $\pm \mid ST/2 \mid$ from the actual frequency shift of the fractional responses.
b. the phase shift of the fractional responses vary by up to $\pi/4\ ST^2$ from the standard compensation.

The additional frequency shift of $\pm \mid ST/2 \mid$ should be judged in relation to the uncertainty $\pm \Delta f/2$ inherently present in the frequency domain representation. If frequency shifts larger than this uncertainty can be encountered we can no longer assign a reliable frequency scale to the display. Therefore we should always ensure

$$\left| ST \right| < \Delta f \Leftrightarrow \left| ST^2 \right| < 1 \Leftrightarrow B^2 < \left| S \right| \qquad (7.6.3)$$

Correct measurement of both magnitude and phase assumes that the contributions from all the fractional responses within the time window are added correctly, i.e. in phase. The satisfaction of this demand also leads to the condition (7.6.3), verifying the results of the more intuitive approach in Section 5.

Conclusion

Based on the general transfer function theory given in Part I of this article we have developed two alternative descriptions of the TDS technique.

In section 5 it is shown that the limitations associated with a TDS measurement can always be expressed as a minimum allowable sweep time. It is characteristic for the TDS technique that this minimum measuring time will depend only on the chosen frequency and time delay windows F and T – and not on the actual response ranges of the device under test. Most other techniques require averaging of several consecutive measurements when measuring in noisy environments. The severe drawbacks imposed by this practice are avoided with TDS where enhanced signal to noise ratio is achieved by simply increasing the sweep time.

Following the system description in section 6 a more sophisticated model for the signal processing is derived in section 7. The analysis involved is regarded as a special correlation technique, where the special properties of the linear sine sweep are utilized. Using this model we find the same limitations as obtained from the intuitive approach in section 5.

We conclude, that whenever the input of a system is accessible for excitation and the signals are corrupted by noise, the TDS technique offers performance equal to or superior to any other technique for measurement of transfer functions. There are no particular limitations whatsoever regarding its ability to resolve the response of a physical system.

References

[1] System Development Type 5842. Brüel & Kjær.

[2] BENDAT, J.S. & PIERSOL, A.G. Engineering Applications of Correlation and Spectral Analysis. *John Wiley & Sons,* 1980.

APPENDIX A

Deriving the phase and group delay from the magnitude response of a minimum phase system

In subsection 3.4 it was stated that the phase response $\theta_m(f)$ of a minimum phase system is derived from the corresponding magnitude response using equation (3.4.12)

$$\theta_m(f) = \frac{2f}{\pi} \int_0^{\infty} \frac{\alpha_m(\phi)}{\phi^2 - f^2}\, d\phi \qquad \text{(A.1)}$$

Initially we evaluate the integral of the coefficient for $\alpha_m(\phi)$,

$$\frac{2f}{\pi} \int \frac{1}{\phi^2 - f^2} d\phi = \frac{-1}{\pi} \ln\left|\frac{\phi + f}{\phi - f}\right| \qquad \text{(A.2)}$$

Using partial integration of (A.1) we obtain

$$\theta_m(f) = \frac{1}{\pi} \int_0^{\infty} \frac{d\alpha_m(\phi)}{d\phi} \cdot \ln\left|\frac{\phi + f}{\phi - f}\right| d\phi - \frac{1}{\pi}\left[\alpha_m(\phi) \ln\left|\frac{\phi + f}{\phi - f}\right|\right]_0^{\infty} \qquad \text{(A.3)}$$

As from (3.4.5) we obtain that $\alpha_m(\phi) \rightarrow -b \ln(f)$ *for* $f \rightarrow \infty$ it is clear that the latter term of (A.3) vanishes completely.

By introducing the logarithmic frequency domain variable $x = \ln(\phi / f)$ we can now rewrite the remaining part of (A.3)

$$\theta_m(f) = \frac{1}{\pi} \int_{-\infty}^{\infty} \frac{d\alpha_m(\phi)}{dx} \ln\left|\frac{e^x + 1}{e^x - 1}\right| dx \qquad \text{(3.4.18), (A.4)}$$

Alternatively we can differentiate with respect to f to determine the group delay

$$\tau_{gm}(f) = \frac{-1}{2\pi^2} \frac{d}{df} \int_0^{\infty} \frac{d\alpha_m(\phi)}{d\phi} \ln\left|\frac{\phi + f}{\phi - f}\right| d\phi$$

$$= \frac{-1}{2\pi^2} \int_0^{\infty} \frac{d\alpha_m(\phi)}{d\phi} \frac{2\phi}{\phi^2 - f^2} d\phi \qquad \text{(A.5)}$$

We can express the integral of the coefficient for $d\alpha_m(\phi)/d\phi$ by

$$\int \frac{2\phi}{\phi^2 - f^2} d\phi = ln \left| (\phi / f)^2 - 1 \right| \qquad \text{(A.6)}$$

where upon partial integration of (A.5) yields

$$\tau_{gm}(f) = \frac{1}{2\pi^2} \int_0^{\infty} \frac{d^2\alpha_m(\phi)}{d\phi^2} \cdot ln \left| (\phi / f)^2 - 1 \right| d\phi$$

$$- \frac{1}{2\pi^2} \left[\frac{d\alpha_m(\phi)}{d\phi} \cdot ln \left| (\phi / f)^2 - 1 \right| \right]_0^{\infty} \qquad \text{(A.7)}$$

As $\alpha_m(f) \rightarrow -b\,ln(f)$ for $f \rightarrow \infty$ implies that $d\alpha_m(f)/df \rightarrow -b/f$ for $f \rightarrow \infty$ it is readily seen that the second term of the expression will not contribute to $\tau_{gm}(f)$.

Also in the group delay expression we will introduce the logarithmic frequency domain variable, x. Using the relationship

$$\frac{d^2\alpha_m(\phi)}{d\phi^2} = \frac{1}{f} e^{-x} \left(\frac{d^2\alpha_m(\phi)}{dx^2} - \frac{d\alpha_m(\phi)}{dx} \right) \frac{dx}{d\phi} \qquad \text{(A.8)}$$

we find after partial integration, that

$$\tau_{gm}(f) = \frac{-1}{2\pi^2 f} \int_{-\infty}^{\infty} \frac{d^2\alpha_m(\varphi)}{dx^2} \cdot ln \left| \frac{e^x + 1}{e^x - 1} \right| dx \qquad \text{(3.4.19), (A.9)}$$

APPENDIX B

Derivation of the TDS delay substitution

With the definitions given in subsection 7.4 equation (7.4.3) can be derived as follows:

$$\forall t \in \left[0, T_s\right]:$$

$$u_+^{\star} \cdot p_+(t) \cdot q_+(t) \cdot r(n,t)$$

$$= \frac{1}{2}\, o^{\star}(t) \cdot l^{\star}(t) \cdot p_+(t) \cdot q_+(t) \cdot r(n,t)$$

$$= \frac{1}{2}\, o^{\star}(t) \cdot e^{-j\pi S t^2} \cdot e^{-j2\pi f_1 t} \cdot e^{j2\pi f_0 t} \cdot e^{-j2\pi (n/T_s) t}$$

$$= \frac{1}{2}\, o^{\star}(t) \cdot \exp\Bigg[-j\pi S\Big[t^2 + 2t\Big((n/T_s) + f_1 - f_0\Big)/S +$$

$$\Big(\Big((n/T_s) + f_1 - f_0\Big)/S\Big)^2 - \Big(\Big((n/T_s) + f_1 - f_0\Big)/S\Big)^2\Big]\Bigg]$$

$$= \frac{1}{2}\, e^{-j2\pi f_a(\tau+\xi-\eta)}\; e^{-j\left(2\pi f_a\left(t-(\tau+\xi-\eta)\right) + \theta_a\right)}$$

$$e^{-j\pi S\left(t-(\tau+\xi-\eta)\right)^2}\; e^{j\pi S(\tau+\xi-\eta)^2}$$

$$= \frac{1}{2}\, e^{-j2\pi f_a(\tau+\xi-\eta)} \cdot l(\tau+\xi-\eta) \cdot l^{\star}\Big(t-(\tau+\xi-\eta)\Big) \cdot o^{\star}\Big(t-(\tau+\xi-\eta)\Big) \qquad \text{(B.1)}$$

APPENDIX C

Derivation of the modified crosscorrelation function obtained with Time Delay Spectrometry

The derivation of $R^{I}_{uy}(\tau)$ given here is based on the assumptions and definitions made in section 7.5. Please refer to this section.

$$R^{I}_{u_+y_+}(\tau) = \frac{1}{T_s} \int_0^{T_s} \Big(y_+(\alpha) \cdot u_+^{\star}(\alpha) \cdot p_+(\alpha) \Big) * h(\alpha) \cdot q_+(\alpha) \cdot r(n,\alpha)\, d\alpha$$

$$= \frac{1}{T_s} \int_0^{T_s} \int_{-\infty}^{\infty} y^+(t) \cdot u_+^{\star}(t) \cdot p_+(t) \cdot q_+(t) \cdot r(n,t) \cdot$$

$$h(\alpha - t) \cdot q_+(\alpha - t) \cdot r(n, \alpha - t)\, dt\; d\alpha$$

$$= \frac{1}{T_s} \int_0^{T_s} \int_{-\infty}^{\infty} g(\gamma) \cdot u_+(t-\gamma)\, d\gamma \cdot \frac{1}{2} e^{-j2\pi f_a(\tau+\xi-\eta)} \cdot I(\tau+\xi-\eta) \cdot$$

$$I^{\star}(t-\tau-\xi+\eta) \cdot o^{\star}(t-\tau-\xi+\eta) \cdot \int_{-t}^{T_s - t} h(\alpha) \cdot e^{j2\pi S(\tau-\eta)\alpha}\, d\alpha\; dt$$

$$= \frac{1}{2\,T_s} e^{j2\pi f_a(\tau+\xi-\eta)} \cdot I(\tau+\xi-\eta) \cdot$$

$$\int_0^{T_s} \int_{t-T_s}^{t} g(\gamma) \cdot \frac{1}{2} I(t-\gamma)\, o(t-\gamma) \cdot I^{\star}(t-\tau-\xi+\eta)\, o^{\star}(t-\tau-\xi+\eta) d\gamma \cdot$$

$$\int_{-\infty}^{\infty} \frac{1}{2} \Big(\operatorname{sgn}(\alpha + t) - \operatorname{sgn}(\alpha + t - T_s) \Big) h(\alpha)\, e^{j2\pi S(\tau-\eta)\alpha}\, d\alpha dt$$

$$= \frac{1}{4T_s} \int_{-T_s}^{T_s} g(\gamma) \cdot e^{-j2\pi f_a \gamma} \cdot e^{j\pi S\gamma^2} \int_{\gamma}^{T_s} e^{j2\pi S(\tau+\xi-\eta-\gamma)t} \cdot$$

$$\int_{-\infty}^{\infty} H\Big(-S(\tau-\eta-\epsilon)\Big) \frac{e^{j2\pi ST_s\epsilon}-1}{j2\pi S\epsilon} e^{-j2\pi St\epsilon} \, d\epsilon \, dt \, d\gamma$$

$$= \frac{1}{4T_s} \int_{-\infty}^{\infty} \int_{-T_s}^{T_s} g(\gamma) \cdot e^{-j2\pi f_a \gamma} \cdot e^{j\pi S\gamma^2}$$

$$\frac{e^{j2\pi ST_s(\tau+\xi-\eta-\epsilon-\gamma)} - e^{j2\pi S\gamma(\tau+\xi-\eta-\epsilon-\gamma)}}{j2\pi S(\tau+\xi-\eta-\epsilon-\gamma)} d\gamma$$

$$H\Big(-S(\tau-\eta-\epsilon)\Big) \cdot \frac{e^{j2\pi ST_s\epsilon}-1}{j2\pi S\epsilon} \, d\epsilon$$

$$= \frac{T_s}{4F^2} \left(\int_{-\infty}^{\infty} g'_{\delta}(\tau+\xi-\eta, \gamma_0) * w_1(\tau+\xi-\eta, \gamma_0) \, d\gamma_0 \cdot \right.$$

$$\left. H\Big(-S(\tau-\eta)\Big) \right) * ww_2(\tau-\eta) \qquad \text{(C.1)}$$

News from the Factory

Studio Microphones Types 4003, 4004, 4006, 4007 and Two Channel Microphone Power Supply Type 2812

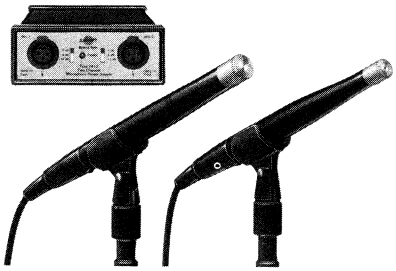

With more than twenty-five years experience in the development and manufacture of precision measurement microphones, Brüel & Kjær has developed a range of four omnidirectional condenser microphones specifically intended for professional studio use. Designated Types 4003/4006 and 4004/4007, two basic microphone designs are offered: Types 4003 and 4006 are acoustically identical, low-noise (15 dB(A)) microphones which differ only in the method of powering. Type 4006 is powered from the standard P48 Phantom system while Type 4003 is powered via B & K Power Supply Type 2812, the advantage being a high ("line-level") balanced, transformerless output. Types 4004 and 4007 are also acoustically identical and are intended for applications requiring a very high-level handling capability ($<1\%$ total harmonic distortion at 148 dB) and extended frequency and phase responses. Type 4007 is Phantom powered while Type 4004 is powered via Power Supply Type 2812. Each Microphone having undergone a thorough quality control procedure is supplied with a calibration chart, which contains the individually measured on-axis frequency response, sensitivity and equivalent noise level of the microphone.

These studio microphones have been designed with particular emphasis on the ability to render a balanced and clean sound image, free from tonal colouration both on- and off-axis. The on-axis response of Types 4003/06 ranges from 20 Hz to 20 kHz ± 2 dB with a very smooth high-frequency roll off. Smaller diameter Types 4004/07 have an on-axis response from 20 Hz to 40 kHz ± 2 dB. Owing to the relatively small cartridge diameters they retain omnidirectivity at high frequencies.

The Microphones are prepolarized condenser microphones utilizing a fixed charge carrying layer which is deposited on the microphone backplate. For dimensional and long-term stability and to ensure a robust construction the cartridge, protection grid and main body housing are manufactured from carefully selected, corrosion resistant materials.

The 2812 is an extremely robust, low-noise power preamplifier and impedance converter with the ability to drive very long cables. The input signal to each of the two channels may be independently attenuated by 0, 6, or 12 dB and channel separation is better than 90 dB.